Inhibition of Epidermal Growth Factor Receptor Tyrosine Kinase Ameliorates Collagen-Induced Arthritis

Christina D. Swanson,*,† Elliot H. Akama-Garren,* Emily A. Stein,*,† Jacob D. Petralia,* Pedro J. Ruiz,* Abdolhossein Edalati,† Tamsin M. Lindstrom,*,† and William H. Robinson*,†

Rheumatoid arthritis (RA) is an autoimmune synovitis characterized by the formation of pannus and the destruction of cartilage and bone in the synovial joints. Although immune cells, which infiltrate the pannus and promote inflammation, play a prominent role in the pathogenesis of RA, other cell types also contribute. Proliferation of synovial fibroblasts, for example, underlies the formation of the pannus, while proliferation of endothelial cells results in neovascularization, which supports the growth of the pannus by supplying it with nutrients and oxygen. The synovial fibroblasts also promote inflammation in the synovium by producing cytokines and chemokines. Finally, osteoclasts cause the destruction of bone. In this study, we show that erlotinib, an inhibitor of the tyrosine kinase epidermal growth factor receptor (EGFR), reduces the severity of established collagen-induced arthritis, a mouse model of RA, and that it does so by targeting synovial fibroblasts, endothelial cells, and osteoclasts. Erlotinib-induced attenuation of autoimmune arthritis was associated with a reduction in number of osteoclasts and blood vessels, and erlotinib inhibited the formation of murine osteoclasts and the proliferation of human endothelial cells in vitro. Erlotinib also inhibited the proliferation and cytokine production of human synovial fibroblasts in vitro. Moreover, EGFR was highly expressed and activated in the synovium of mice with collagen-induced arthritis and patients with RA. Taken together, these findings suggest that EGFR plays a central role in the pathogenesis of RA and that EGFR inhibition may provide benefits in the treatment of RA. ***The Journal of Immunology*****, 2012, 188: 3513–3521.**

Rheumatoid arthritis (RA) is an autoimmune disease characterized by synovial inflammation and joint destruction. T cells, B cells, macrophages, and dendritic cells infiltrate the inflamed synovium and drive disease by producing cytokines and autoantibodies (1). For this reason, current biological therapies for RA (such as TNF inhibitors, abatacept, rituximab, and tocilizumab) directly target these immune cells and proinflammatory cytokines, dampening the immune response (2). However, these therapies also increase the risk of infections such as tuberculosis, indicating that other therapies, especially ones targeting nonimmune cells, may be beneficial (2). In addition to the typical immune cells, synovial fibroblasts, endothelial cells, and osteoclasts have been highlighted for their roles in promoting RA. Synovial fibroblasts form pannus and produce inflammatory mediators and chemokines that promote immune cell infiltration of the synovium. Proliferation of endothelial cells results in neovascularization, which supports the growth of the pannus by supplying it with nutrients and oxygen (3), and osteoclasts mediate adjacent bone destruction (4).

A recent case study described the prolonged remission of RA symptoms in an RA patient who was treated for head and neck cancer with focal radiation and cetuximab, a mAb against epidermal growth factor receptor (EGFR) (5). Moreover, adenoviral expression of soluble herstatin, an alternative splice variant of erythroblastic leukemia viral oncogene homolog (ErbB)2 that naturally inhibits dimerization of ErbB receptors, effectively reduced the severity of collagen-induced arthritis (CIA), a mouse model of RA (6). Similarly, RB200, a ligand trap that inhibits responses from EGFR, ErbB2, and ErbB3, reduced CIA severity (7). These findings suggest that inhibiting EGFR may be beneficial in RA.

EGFR is a widely expressed member of the ErbB family of tyrosine kinase receptors (8) and is overexpressed in many tumors (8). Activation of EGFR promotes survival, proliferation, cytokine production, cell adhesion, blood vessel recruitment, and invasion depending on the cell type (8). Similar to a tumor, RA synovium is hyperplastic, invasive, and expresses EGFR. Specifically, EGFR is expressed on RA fibroblast cell lines and on the vascular endothelial cells and subsynovial fibroblasts of certain RA patients (9, 10). Moreover, levels of EGFR ligands, such as EGF, amphiregulin, or TGF-α, are significantly higher in synovial fluid, serum, or synovium of RA patients than in that of osteoarthritis patients or noninflammatory controls (9, 11, 12).

In this study, we elucidate the role of EGFR in RA. We show that levels of EGF ligands are abnormally high in the serum of RA patients and that EGFR is expressed and activated in RA synovial tissue. Moreover, we demonstrate that erlotinib hydrochloride (Tarceva), a small-molecule EGFR inhibitor that is Food and Drug

*Division of Immunology and Rheumatology, Department of Medicine, Stanford University, Stanford, CA 94305; and †Veterans Affairs Palo Alto Health Care System, Palo Alto, CA 94304

Received for publication September 19, 2011. Accepted for publication January 10, 2012.

This work was supported by National Institutes of Health National Heart Lung and Blood Institute Contract N01-HV-00242 (to W.H.R.), National Institutes of Health/National Institute of Arthritis and Musculoskeletal and Skin Diseases Grant R01 AR-054822 (to W.H.R.), and National Institutes of Health Training Grant 5 T32 AI07290 for Molecular and Cellular Immunobiology (to C.D.S.).

Address correspondence and reprint requests to Christina D. Swanson or William H. Robinson, Veterans Affairs Palo Alto Health Care System, Building 101, Room C4-185, 3801 Miranda Avenue, Palo Alto, CA 94304-1207. E-mail addresses: christina.d.swanson@gmail.com (C.D.S.) or wrobins@stanford.edu (W.H.R.)

The online version of this article contains supplemental material.

Abbreviations used in this article: CIA, collagen-induced arthritis; COX-2, cyclooxygenase-2; EGF, epidermal growth factor; EGFR, EGF receptor; ERBB, erythroblastic leukemia viral oncogene homolog; FLS, fibroblast-like synoviocyte; HB-EGF, heparin-binding epidermal growth factor-like growth factor; HPRT1, hypoxanthine phosphoribosyltransferase 1; LDH, lactate dehydrogenase; MMP, matrix metalloprotease; PDGFbb, platelet-derived growth factor bb; RA, rheumatoid arthritis; RANKL, receptor activator for NF-κB ligand; TRAP, tartrate-resistant acid phosphatase; VEGF, vascular endothelial growth factor.

www.jimmunol.org/cgi/doi/10.4049/jimmunol.1102693

Downloaded from www.jimmunol.org on April 4, 2012

Administration approved for the treatment of metastatic non-small cell lung cancer (13), can attenuate CIA. Findings from our in situ and in vitro studies suggest that erlotinib ameliorates autoimmune arthritis by inhibiting the EGFR-dependent proliferation and cytokine production of synovial fibroblasts, proliferation of endothelial cells, and formation of osteoclasts.

Materials and Methods

Serum and joint tissue samples

Serum samples were collected from RA patients who met the 1987 American College of Rheumatology criteria and from healthy individuals under protocols approved by the Stanford University Institutional Review Board. Joint tissue was collected from RA patients undergoing knee arthroplasty and was snap-frozen in OCT freezing media.

Reagents

For animal studies, we used erlotinib tablets (OSI) purchased from the Stanford Inpatient Pharmacy Service. Erlotinib tablets were formulated as a fine suspension with 0.5% (w/v) hydroxypropyl methyocellulose (Dow) and 0.1% (v/v) Tween 80 in distilled water. For in vitro studies, we used 99% pure, chemically synthesized erlotinib (LC Laboratories) stored as a 100 mM stock solution at −20°C in DMSO. PD153035 (Tocris Bioscience) was stored as a 10 mM stock solution at −20°C in DMSO. For all studies, we used recombinant murine EGF, murine platelet-derived growth factor bb (PDGFbb), human EGF, human vascular endothelial growth factor (VEGF), murine M-CSF, and murine receptor activator for NF-κB ligand (RANKL) (PeproTech) reconstituted in water.

Immunohistochemistry

Seven-micrometer sections of synovial tissue from patients with RA were fixed in 4% (v/v) paraformaldehyde, permeabilized with Triton X-100, and probed with Abs against total EGFR (clone LA-1; Millipore) or EGFR phosphorylated at tyrosine 1068 (p-EGFR [Y1068]; Abcam). Hind limbs of mice with CIA were fixed in formalin and embedded as described in the histology section. Seven-micrometer sections of mouse paws were rehydrated, subjected to Ag retrieval using ficin solution (Invitrogen), and probed with Abs against total EGFR (Rockland), p-EGFR (Y1068) (Abcam), von Willebrand factor (Millipore), or tartrate-resistant acid phosphatase (TRAP) (Abcam). Staining was developed using a Vectastain Elite ABC kit for mouse and rabbit IgG (Vector Laboratories). To quantify the number of vessels and osteoclasts in the mouse paw, we took images of the ankle and the calcaneous/cuboid joint, respectively, and counted the vessels or cells per square millimeter. Images and quantification were performed in a blinded manner.

CIA and K/BxN studies

CIA was generated in 6- to 8-wk-old male DBA/1 mice (The Jackson Laboratory) weighing ~20 g. Mice were used under protocols approved by the Administrative Panel on Laboratory Animal Care and in accordance with National Institutes of Health guidelines. For the induction of CIA, mice were first immunized with a s.c. tail injection of 100 μg bovine CII (Chondrex) emulsified in 100 μl CFA containing 250 μg/mouse heat-killed *Mycobacterium tuberculosis* H37Ra (BD Biosciences). Twenty-one days after the primary immunization, mice were boosted by s.c. injection at the base of the tail with 100 μg bovine CII emulsified in 100 μl IFA. Mice were assessed daily for signs of inflammatory arthritis. As each mouse reached a total paw score between 2 and 4, it was randomly assigned to a treatment group. Arthritis severity was assessed using both a visual scoring system and paw thickness measurements. For the visual scoring system, each mouse could have a maximal score of 16 because each limb was given a score of 0–4. Grade 0 indicated no swelling or erythema; grade 1, mild swelling and erythema or digit inflammation; grade 2, moderate swelling and erythema confined distal to the midpaw; grade 3, more pronounced swelling and erythema with extension to the ankle; and grade 4, severe swelling, erythema, and joint rigidity of the ankle, foot, and digits. Paw thickness was determined by measuring the thickness of the hind paws above the metatarsal region using 0- to 10-mm calipers. As each mouse reached a total paw score between 2 and 4, it was randomly assigned to a treatment group. Upon randomization into a treatment group, mice were given 0.2 ml vehicle, 10 mg/kg erlotinib, or 50 mg/kg erlotinib twice daily by oral gavage using a 1-ml syringe and a 20-gauge gavage needle (Fisher Scientific). All mouse groups were treated until inflammation in the vehicle-treated mice peaked and began to decrease, as assessed by visual score and paw thickness. At that time, feet and ankles were collected in formalin for histology.

K/BxN serum-transfer arthritis was induced in BALB/c mice by dual injections of 50 μl KRN serum diluted 1:1 in 1× PBS on day 0 and day 2. Mice were treated with either vehicle or 50 mg/kg erlotinib twice daily by oral gavage. Mice were scored as described above.

Histopathology

Mouse hind limbs were fixed in formalin, decalcified in Cal-Ex II (Fischer Scientific), and embedded in paraffin. Sections were stained with H&E and scored by an investigator blinded to the treatment group. Sections were evaluated for synovitis, pannus formation, and bone and/or cartilage destruction using a previously described scoring system: grade 0, normal; grade 1, mild inflammation, mild hyperplasia of the synovial lining layer, mild cartilage destruction without bone erosion; grades 2–4, increasing degrees of inflammatory cell infiltrates, synovial lining hyperplasia, and pannus formation and cartilage and bone destruction (14).

Isolation and stimulation of synovial fibroblasts

Synovial fibroblasts were isolated from remnant pannus obtained from RA patients during knee arthroplasty, as previously described (14), and cultured in RPMI 1640 containing 10% FCS, 2 mM L-glutamine, 100 U/ml penicillin, and 100 μg/ml streptomycin sulfate at 37°C, 5% CO_2. Cells were used for experiments between passages five and eight and exhibited characteristic fibroblast appearance. Moreover, cells were checked at passage six for purity and did not exhibit staining above background for CD3, CD14, CD20, and CD11c (Supplemental Fig. 1). For experiments, 1×10^3 cells/cm^2 were plated in media containing 5% FBS, RPMI 1640, and penicillin/streptomycin and allowed to adhere for 24 h. Media were replenished, cells were pretreated with erlotinib or PD153035 for 30 min, and EGF or PDGFbb was added to cells for another 48 h. Supernatants were collected after 48 h for ELISA analysis.

Endothelial cell stimulation

HUVEC (Lonza) were cultured in endothelial growth media-2 (Lonza) on plates coated with 10 μg/cm^2 rat tail collagen I (Sigma-Aldrich). To evaluate HUVEC proliferation, we plated cells at a density of 1×10^3 cells/cm^2 in complete media and allowed them to adhere overnight. Cells were then washed with 1× PBS and incubated with reduced-serum media containing endothelial basal media-2 (Lonza), 1% FBS, 2 mM L-glutamine, 100 U/ml penicillin, and 100 μg/ml streptomycin sulfate at 37°C, 5% CO_2 for 24 h. Cells were pretreated with erlotinib for 30 min, and EGF or VEGF was added for 72 h.

Proliferation assays

BrdU was added during the last 24 h incubation to evaluate synovial fibroblast and HUVEC proliferation. BrdU incorporation was assessed as a marker of proliferation by using a BrdU cell proliferation assay (Calbiochem) according to the manufacturer's instructions.

ELISAs

Levels of EGF, betacellulin (PeproTech), amphiregulin, heparin-binding epidermal growth factor-like growth factor (HB-EGF), and TGF-α (R&D Systems) were determined by ELISA in serum samples diluted 1:2 to 1:200 in assay diluent. Levels of VEGF, IL-8, MCP-1 (PeproTech), and matrix metalloprotease (MMP)-3 (R&D Systems) were determined by ELISA in supernatants collected from synovial fibroblast cultures 48 h after stimulation. For IgG ELISAs, plates were coated with 100 μg/ml bovine collagen II. Mouse serum diluted 25-fold was then added, followed by anti–IgG1-HRP or anti–IgG2a-HRP (SouthernBiotech) diluted 10,000 fold. Absorption was read at 450 nm.

Osteoclast assays

Bone marrow cells were isolated from naive, 7-wk-old DBA/1J mice. Twenty-four hours after being isolated, undifferentiated (nonadherent) cells were collected and replated at 15×10^3 cells/cm^2. Cells were stimulated with 40 ng/ml M-CSF (PeproTech) in complete α-MEM for 3 d. Differentiation medium containing 40 ng/ml M-CSF and 100 ng/ml RANKL (PeproTech) was then added for another 3–4 d, and osteoclast formation was monitored visually. For these studies, culture medium was refreshed every 2 d. Erlotinib or PD153035 was added to the cultures at the specified concentrations at the beginning of the differentiation period. For identification of TRAP$^+$ cells, cells were washed with 1× PBS and stained using the acid phosphatase leukocyte kit (Sigma-Aldrich). Eight photographs of each well at ×40 and ×100 were analyzed in a blinded manner. The number of osteoclasts per picture and the number of nuclei per osteoclast were counted. ImageJ was used to calculate the surface area of the

Downloaded from www.jimmunol.org on April 4, 2012

osteoclasts formed. For measurement of TRAP enzyme activity, cells were lysed at 4°C in a buffer containing 90 mM citrate, 0.1% Triton X-100, and 80 mM sodium tartrate for 10 min. Substrate solution consisting of 20 mM *p*-nitrophenyl phosphate was then added to the wells for 1 h at room temperature. The reaction was stopped by the addition of 0.5 M NaOH, and plates were read at 405 nm. For bone resorption assays, osteoclasts were grown on dentine discs (Boldon) for 3 d with 40 ng/ml M-CSF and 6 d with 40 ng/ml M-CSF, 100 ng/ml RANKL, and erlotinib. Media was changed every two days. After 9 d, discs were washed with distilled water, gently rubbed with a cotton swab to remove attached cells, and stained with toluidine blue. Resorbed areas were photographed and analyzed using ImageJ software.

Quantification of mRNA expression

RNA isolation was performed using the RNeasy kit (Qiagen), and cDNA was made using the qScript cDNA synthesis kit (VWR). Real-time PCR was performed using PerfeCTa SYBR 2× mix (VWR). Primers, purchased from IDT, were as follows: human cyclooxygenase-2 (*COX-2*), forward 5′-CCGGGTACAATCGCACTTAT-3′, reverse 5′-GGCGCTCAGCCATACAG-3′; human *GAPDH*, forward 5′-GAAGGCTGGGGCTCATTT-3′, reverse 5′-ATGGTTCACACCCATGACG-3′; murine *Acp5*, forward 5′-GCTGGAAACCATGATCACCT-3′, reverse 5′-GCAAACGGTAGTAAGGGCTG-3′; murine *Ctsk*, forward 5′-GCCGTGGCGTTATACATACA-3′, reverse 5′-CTTCCAATACGTGCAGCAGA-3′; murine *Fos*, forward 5′-TGGCACTAGAGACGGACAGA-3′, reverse 5′-TCCTACTACCATTCCCCAGC-3′; murine hypoxanthine phosphoribosyltransferase 1 (*Hprt1*), forward 5′-TGTTGTTGGATATGCCCTTG-3′, reverse 5′-TGGCAACATCAACAGGACTC-3′; murine *Itgb3*, forward 5′-CGCCTC GTGTGGTACAGAT-3′, reverse 5′-AGTGGCCGGGACAACTCT-3′; murine *Mmp3*, forward 5′-AGCCTT GGCTGAGTGGTAGA-3′, reverse 5′-CGATGATGAACGATGGACAG-3′; murine *Mmp9*, forward 5′-CTGTCGGCTGTGGTTCAG T-3′, reverse 5′-AGACGACATAGACGGCATCC-3′; murine *Mmp14*, forward 5′-GTGAGCGTTGTGTGTGGGTA-3′, reverse 5′-CCCAAGGCAGCAACTTCAG-3′; murine *Nfatc1*, forward 5′-AATTAGGAGTGGGGGATCGT-3′, reverse 5′-ATCCAACCCAACTCGCCT-3′. *COX-2* expression was normalized to *GAPDH* levels, and murine gene expression was normalized to *Hprt1* levels.

Western blotting

Cells were serum starved in serum-free media for 3 h prior to stimulation. Whole-cell lysates were generated using a buffer containing 1% NP-40 (Sigma-Aldrich), 0.1% SDS (Fluka), 0.5% sodium deoxycholate (Sigma-Aldrich), 10 mM EDTA (Promega), and 1:100 Halt protease and phosphatase inhibitor cocktail (Thermo Scientific). Lysates were analyzed using standard immunoblotting procedures. Briefly, lysates were separated on 4–12% Bis-Tris gels (Bio-Rad), transferred to polyvinylidene difluoride membranes, blocked with 5% (w/v) BSA or milk, and probed with primary and secondary Abs in BSA or milk. Signal was detected with SuperSignal West Femto chemiluminescent substrate (Pierce Biotechnology). Abs used were against EGFR (Rockland), p-EGFR (Y1068) (Abcam), Akt1 (Cell Signaling Technology), p-Akt (S473) (Cell Signaling Technology), Erk1/2 (Cell Signaling Technology), and p-Erk1/2 (T202, Y204) (Cell Signaling Technology).

Flow cytometry

Human PBMCs and RA synovial fibroblasts were stained with Abs including CD3-PE, CD20-PerCP-Cy5.5, and CD11c-PE (BD Biosciences) and CD14-PeCy7 (eBioscience). Samples were analyzed on a BD LSRFortessa (BD Biosciences).

Cell death assays

Synovial fibroblasts, HUVEC, and osteoclasts were treated with erlotinib or PD153035 for 24 h in the same media and at the same treatment concentrations as used in the cytokine, proliferation, and osteoclast formation assays. Tween 20 was added for the last hour to induce a loss of membrane integrity and release of lactate dehydrogenase (LDH). Cell supernatants were analyzed using an LDH cytotoxicity assay kit (Cayman Chemical). Briefly, supernatants were incubated for 30 min at room temperature with a reaction buffer containing LDH diaphorase, NAD^+, lactic acid, and tetrazolium salt. Absorbance was then read at 490 nm.

Statistical analysis

Visual arthritis scores, paw thicknesses, and histology scores were analyzed by the Mann–Whitney *U* test using GraphPad InStat version 3.0 (GraphPad Software). All other data were analyzed using an unpaired two-tailed Student *t* test (GraphPad Software).

Results

Levels of EGF are increased in RA serum

Which EGFR ligands play a role in RA are unclear, with differing reports each suggesting that EGF, TGF-α, or amphiregulin is the important EGFR ligand (9, 11, 12). We measured the concentration of the five best characterized EGFR ligands in serum from RA patients and normal controls. Levels of EGF and betacellulin were significantly higher in sera from RA patients than in that from healthy individuals (Fig. 1A, Supplemental Fig. 2A). In contrast, serum levels of TGF-α, amphiregulin, or HB-EGF did not differ significantly between the two groups (Supplemental Fig. 2B–D). Thus, there is an increased capacity for activation of EGFR signaling in patients with RA.

EGFR is expressed in RA and CIA joint tissue

We next examined whether the synovial tissue of patients with RA and of mice with CIA express EGFR, and whether the EGFR in these tissues is activated. We found that RA synovial lining expresses high levels of both total EGFR and tyrosine 1068-phosphorylated (Y1068) EGFR, the activated form of EGFR (Fig. 1B–D). Deeper within the RA synovial tissue, EGFR was expressed around high-endothelial venules and blood vessels (Fig. 1C). Likewise, EGFR and p-EGFR (Y1068) were highly expressed in areas of synovitis and around vessels in joint tissues of mice with CIA (Fig. 1E, 1F). Thus, EGFR is expressed and activated in synovial tissue in RA, as well as in the CIA model of RA.

EGFR inhibition reduces the severity of CIA

To investigate the role of EGFR in CIA, we administered 10 or 50 mg/kg erlotinib twice daily to mice with established CIA. These doses of erlotinib produce plasma concentrations in the same range as those achieved with human dosing (15, 16). Erlotinib treatment dose-dependently reduced the visual arthritis score and paw

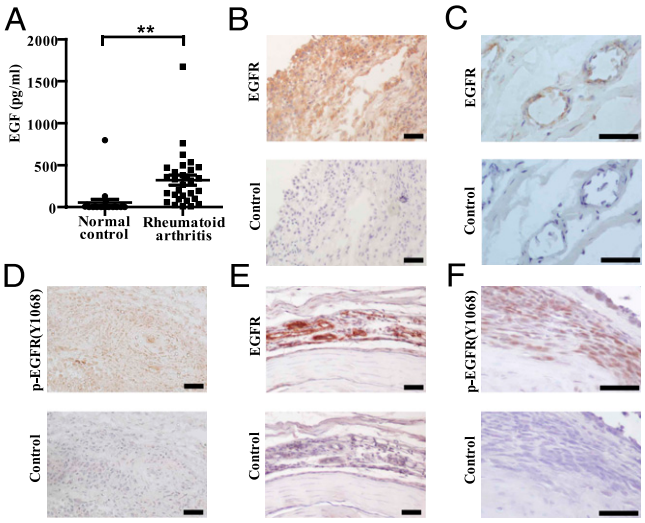

FIGURE 1. EGF and EGFR are expressed in RA and CIA. (**A**) EGF concentration was measured in serum from normal controls (n = 20) and RA patients (n = 30) by ELISA. $^{**}p < 0.01$. RA synovial tissue was sectioned and examined for EGFR staining (**B**) in the synovial lining and (**C**) in the subsynovial tissue. RA synovial tissue was examined for (**D**) p-EGFR (Y1068) expression. (**E**) Paws from mice with CIA (score 4) were stained for EGFR and (**F**) p-EGFR (Y1068). Images represent areas of pannus surrounding the bone next to inflammatory foci. (B–F) Control sections indicate adjacent sections stained with appropriate isotype control Abs. (A–C) Data represent two experiments. (E and F) Data represent at least four experiments. Scale bars, 50 μm.

Downloaded from www.jimmunol.org on April 4, 2012

thickness of mice with CIA (Fig. 2A, 2B). Histologically, it dose-dependently reduced the degree of pannus formation, synovitis, and cartilage and bone erosion in the paws of mice with CIA (Fig. 2C, 2D). This was not accompanied by a significant change in the IgG1 or IgG2a titers (Supplemental Fig. 3A, 3B). Similarly, erlotinib treatment also reduced the severity of disease in the K/BxN serum-transfer model (Supplemental Fig. 3C). Thus, erlotinib, at pharmacologically relevant doses, attenuates autoimmune arthritis in mice.

Erlotinib reduces EGF-induced synovial fibroblast proliferation and cytokine production

To elucidate erlotinib's mechanism of action in treating autoimmune arthritis, we first examined its effects on synovial fibroblasts derived from RA patients. In RA, synovial fibroblasts become hyperplastic and invade the surrounding bone and cartilage, forming the pannus (17). EGFR ligands may increase the mitogenic capacity of synovial fibroblasts (9, 18–21), and erlotinib-induced attenuation of CIA was associated with reduction in pannus formation (Fig. 2C, 2D). We therefore tested erlotinib's effect on EGF-induced proliferation of synovial fibroblasts. We concurrently tested the effect of PD153035, another small-molecule inhibitor of EGFR. To assess the specificity of erlotinib, we also tested erlotinib's effect on synovial fibroblast proliferation induced by PDGFbb, which is known to promote synovial fibroblast proliferation and cytokine production through PDGFR, rather than EGFR (14). Erlotinib and PD153035 reduced the proliferation induced by EGF, but not that induced by PDGFbb (Fig. 3A).

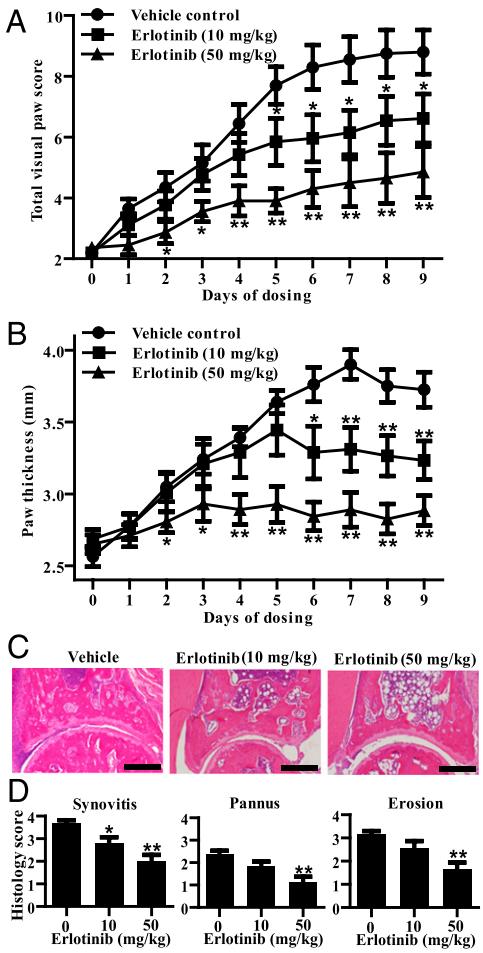

FIGURE 2. Erlotinib treatment ameliorates CIA. Following the development of arthritis, DBA1/J mice with CIA were randomly enrolled in a treatment group when they reached a mean visual arthritis score between 2 and 4. Mice were administered vehicle (n = 10), 10 mg/kg erlotinib (n = 12), or 50 mg/kg (n = 12) erlotinib twice daily by oral gavage. (**A**) Arthritis severity was assessed using a visual arthritis scoring system and (**B**) caliper measurements of paw thickness. Data represent one experiment of at least three independent experiments. (**C**) Representative images of paw sections and (**D**) blinded histological scores of synovitis, pannus formation, and bone and cartilage erosion. Scale bars, 300 μm. Groups were compared at each time point using a Mann–Whitney analysis comparing erlotinib-treated mice to vehicle-treated mice. Error bars indicate ± SEM. $*p < 0.05$, $**p < 0.01$.

EGFR ligands may also stimulate the production of proinflammatory cytokines by synovial fibroblasts (9, 20). We found that EGF induces RA synovial fibroblasts to produce VEGF, IL-8, MCP-1, and MMP-3, and concurrent erlotinib treatment reduced the production of these factors (Fig. 3B–E). All of these EGF-induced cytokines are implicated in RA: VEGF drives angiogenesis (22); IL-8 promotes neutrophil infiltration into the joint space (23); MCP-1 promotes the infiltration of monocytes into the synovium (24); and MMP-3 aids the destruction of cartilage (25).

Treating cells with erlotinib or PD153035 did not induce the release of LDH, indicating that erlotinib's effect on proliferation and cytokine production was not due to the induction of cell death (Supplemental Fig. 4A). Thus, erlotinib can reduce not only proliferation but also cytokine production of synovial fibroblasts (Fig. 3A–E), indicating that erlotinib may directly reduce pannus formation and indirectly reduce angiogenesis and synovitis by acting on these cells.

We found that erlotinib inhibited the EGF-induced phosphorylation of EGFR, as well as the EGF-induced phosphorylation of Akt and Erk1/2 (Fig. 3F), kinases that mediate two different signaling pathways downstream of EGFR (8). These findings confirm that erlotinib suppresses proliferation and cytokine production by inhibiting EGFR signaling.

Erlotinib reduces EGF-induced endothelial cell proliferation and COX-2 expression

As we show in Fig. 1, endothelial cells in RA and CIA synovium express EGFR. Blood vessels, which are lined with endothelial cells, increase in number in RA synovium as compared with osteoarthritis or healthy synovium (26). Targeting the formation of these blood vessels in RA is hypothesized to have three beneficial consequences: it may reduce the growth of the synovium by decreasing the blood supply that provides nutrients, decrease the inner blood-vessel wall surface area for lymphocyte ingress from the blood into the synovium, and diminish the production of chemoattractants by the endothelial cells (3). Interestingly, EGF and HB-EGF have been shown to promote angiogenesis by increasing endothelial cell proliferation or migration (27–30). To determine whether erlotinib affects neoangiogenesis in CIA, we quantified the number of blood vessels per square millimeter in the ankle of mice treated with vehicle or erlotinib, by staining paw sections for von Willebrand factor. We found that the attenuation of CIA was associated with a reduction in the number of blood vessels formed in the ankles of erlotinib-treated mice, indicating the erlotinib reduces neoangiogenesis in vivo (Fig. 4A, 4B). Furthermore, we show that erlotinib markedly suppresses EGF-induced, but not VEGF-induced, proliferation of HUVEC in vitro, as does PD153035 (Fig. 4D).

COX-2 inhibitors can reduce swelling and pain in the joints of RA patients (31), and COX-2 expression is significantly greater in endothelial cells in RA synovium than in osteoarthritis synovium (32). Moreover, angiogenesis is dependent on COX-2 activity, as COX-2–specific inhibitors strongly reduce tube formation (33).

Downloaded from www.jimmunol.org on April 4, 2012

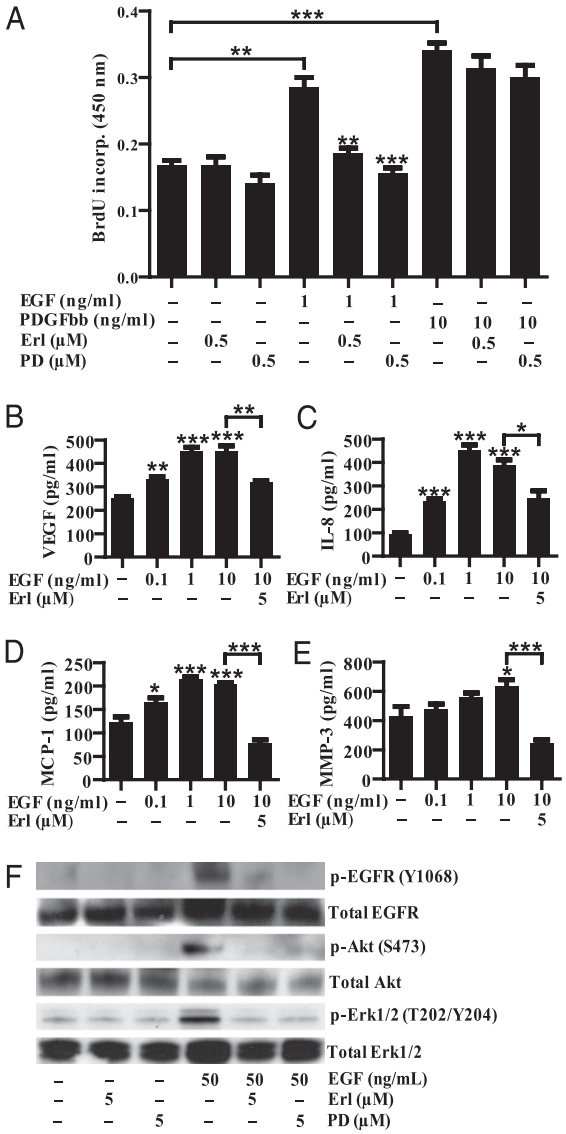

FIGURE 3. Erlotinib reduces RA synovial fibroblast proliferation and cytokine production. (**A**) RA synovial fibroblasts were stimulated with EGF (1 ng/ml) or PDGFbb (10 ng/ml) and concurrently treated with erlotinib (0.5 μM) or PD153035 (0.5 μM). After 48 h incubation, proliferation was analyzed by BrdU incorporation. (**B–E**) RA synovial fibroblasts were stimulated with increasing concentrations of EGF and concurrently treated with erlotinib (5 μM). After a 48-h incubation, the concentrations of (B) VEGF, (C) IL-8, (D) MCP-1, and (E) MMP-3 were determined by ELISA. Data represent one experiment of at least three independent experiments. $*p < 0.05$, $**p < 0.01$, $***p < 0.001$. Error bars indicate ± SEM. (**F**) Cells were pretreated with erlotinib (5 μM) or PD153035 (5 μM) for 30 min, stimulated with EGF (50 ng/ml) for 5 min, and cell lysates were examined via Western blotting. Data represent one experiment of at least three independent experiments. PD, PD153035.

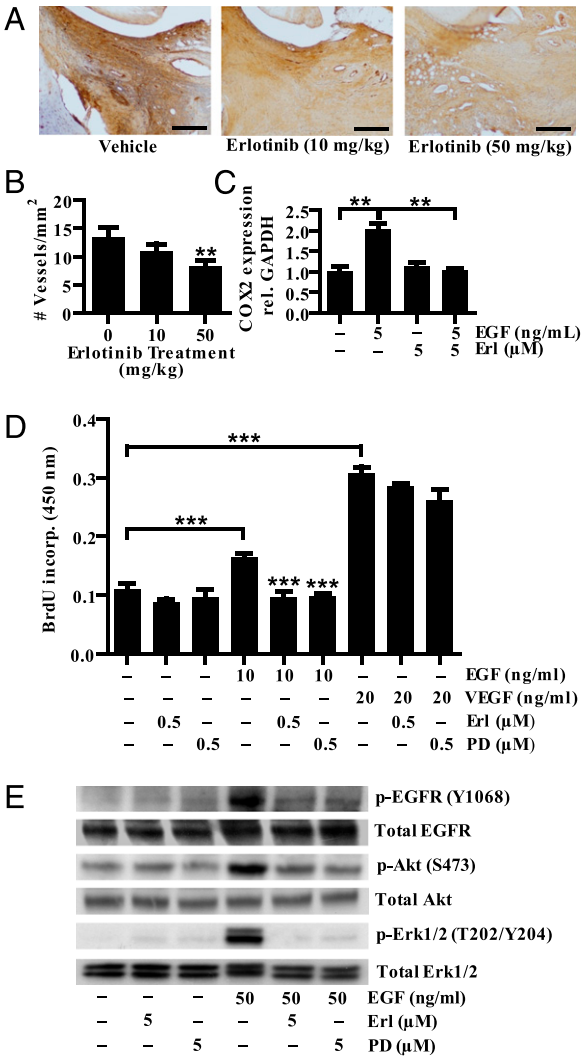

FIGURE 4. Erlotinib inhibits HUVEC proliferation and COX-2 expression. (**A**) Mice with CIA were treated with vehicle or 10 or 50 mg/kg erlotinib twice daily by oral gavage. Paws were collected, sectioned, and stained for von Willebrand factor (VWF). Scale bars, 150 μm. (**B**) The number of VWF-positive vessels in the ankle was quantified per square area for each treatment group. $**p < 0.01$. (**C**) HUVEC were stimulated with 5 ng/ml EGF for 45 min with or without concurrent treatment with 5 μM erlotinib. Cells were collected in TrIzol and RT-PCR was performed to determine COX-2 mRNA expression. (**D**) HUVEC were stimulated with EGF (10 ng/ml) or VEGF (20 ng/ml) and treated with either erlotinib (0.5 μM) or PD153035 (0.5 μM). Proliferation was measured by BrdU incorporation. (**E**) Cells were pretreated with erlotinib (5 μM) or PD153035 (5 μM) for 30 min, stimulated with EGF (50 ng/ml) for 5 min, and cell lysates were examined via Western blotting. (C and D) Data represent one experiment of at least three independent experiments. Error bars indicate ± SEM. $**p < 0.01$, $***\ p < 0.001$.

Previous studies have indicated that EGF induces COX-2 expression in RA synovial fibroblasts (21). We found that erlotinib inhibits the EGF-induced expression of COX-2 in HUVEC, suggesting that erlotinib may be reducing angiogenesis in vivo by modulating COX-2 expression in endothelial cells (Fig. 4C).

Erlotinib inhibited the EGF-induced phosphorylation of EGFR, as well as the EGF-induced phosphorylation of Akt and Erk1/2 in HUVEC (Fig. 4E), signifying that erlotinib suppresses HUVEC proliferation and COX-2 expression by inhibiting EGFR signaling. Erlotinib and PD153035 did not induce LDH release after 24 h treatment (Supplemental Fig. 4B), indicating that their suppression of HUVEC proliferation is not due to cell death.

Erlotinib reduces osteoclastogenesis

RA and CIA are characterized by the progressive destruction of bone and cartilage in the synovial joints (34, 35). This destruction is mediated by osteoclasts, which resorb mineralized bone and cartilage (4). Numerous osteoclasts are found in and adjacent to the inflamed synovium and are thought to derive from monocyte/macrophage lineage cells in the synovium (4). Because erlotinib treatment reduced the erosion of bone and cartilage in the joints of

Downloaded from www.jimmunol.org on April 4, 2012

mice with CIA (Fig. 2), we compared the number of osteoclasts in the paws of CIA mice treated with vehicle and those treated with erlotinib. To this end, we performed immunohistochemical analysis for the expression of tartrate-resistant acid phosphatase (TRAP), a characteristic of osteoclasts. As with cartilage and bone erosion, there were more TRAP$^+$ cells in vehicle-treated than in erlotinib-treated mice. In fact, erlotinib reduced the number of TRAP-positive cells in a dose-dependent fashion (Fig. 5A). We next asked whether erlotinib could directly reduce the in vitro formation of osteoclasts, which we defined as TRAP$^+$ cells with three or more nuclei. Erlotinib significantly reduced the number of osteoclasts formed from bone marrow-derived monocytes; it also reduced the size of the osteoclasts (Fig. 5B–D). Erlotinib treatment significantly decreased the expression of four genes characteristic of osteoclasts: *Acp5*, which encodes TRAP; *Ctsk*, which encodes cathepsin K; *Itgb3*, which encodes β_3-integrin; and *Nfatc1*, which encodes NF of activated T cells, cytoplasmic 1 (Fig. 5E) (36). Erlotinib treatment also reduced the expression of several MMPs, including *Mmp3*, *Mmp9*, and *Mmp14*, which mediate breakdown of the nonmineralized parts of the bone (Fig. 5E). Moreover, treatment with erlotinib significantly decreased osteoclast-mediated bone resorption (Fig. 5F) and did not alter LDH release (Supplemental Fig. 4C). This indicates that erlotinib inhibits the formation of osteoclasts from mononuclear cells. Taken together, this showed that EGFR inhibition reduces osteoclastogenesis.

TNF promotes osteoclastogenesis both directly and indirectly by promoting RANKL expression and binding TNF-α receptor type 1 on osteoclasts (4). To determine whether EGF promotes osteoclastogenesis directly, we treated the bone marrow-derived monocytes with EGF in the presence of osteoclast differentiation media containing a reduced concentration of RANKL, and then measured TRAP enzymatic activity and quantified the number of osteoclasts formed. A reduced concentration of RANKL was used

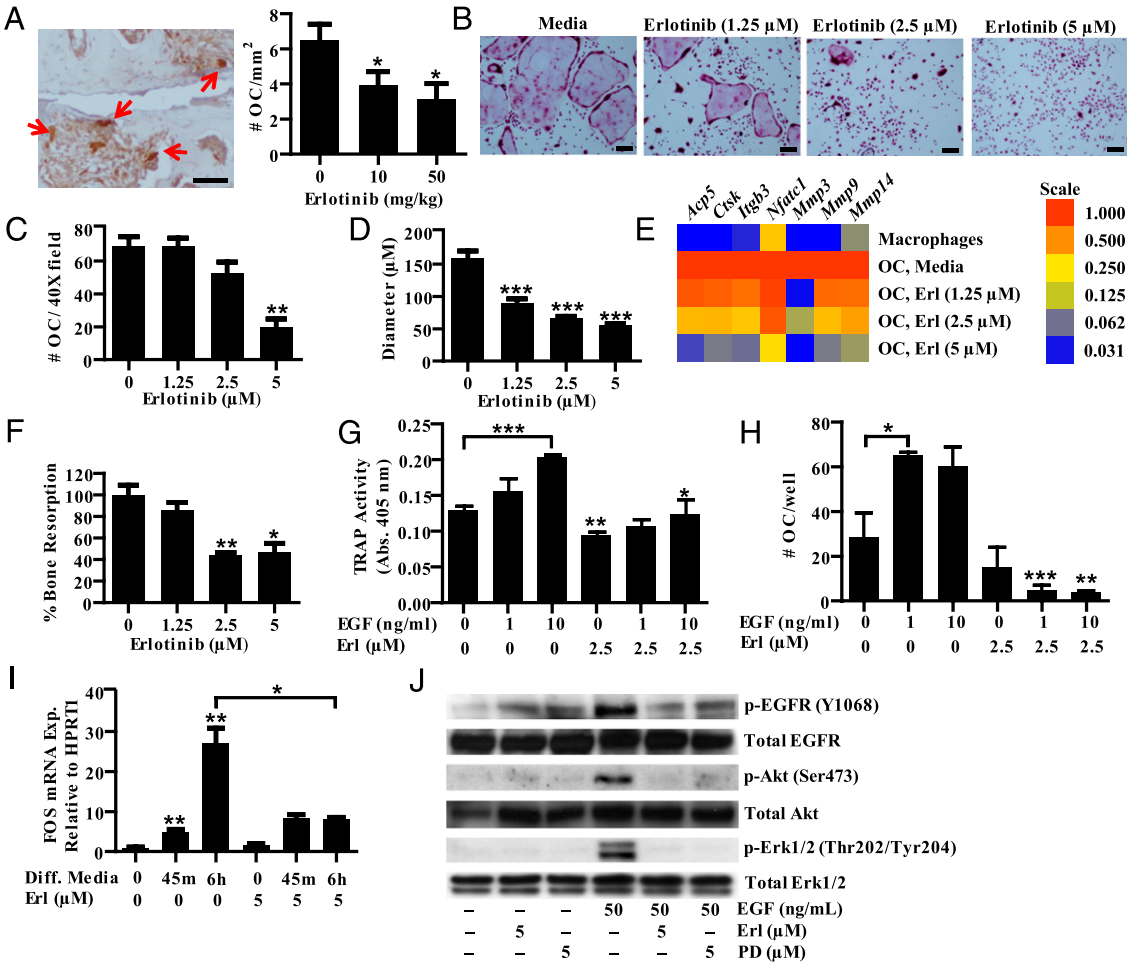

FIGURE 5. Erlotinib inhibits osteoclastogenesis. (**A**) Paw sections from CIA mice treated with vehicle or erlotinib were stained for TRAP. Arrows indicate osteoclasts, defined as large, TRAP$^+$ cells adjacent to bone. The number of osteoclasts was quantified for each treatment group. (**B–D**) Osteoclasts were treated with erlotinib during the differentiation period and stained for TRAP. (B) Representative images were taken, and the (C) number and (D) relative diameter of osteoclasts was determined using ImageJ analysis. For quantification, osteoclasts were defined as TRAP$^+$ cells with three or more nuclei. (**E**) Expression of osteoclast-specific genes and MMPs was quantified in macrophages and osteoclasts treated with erlotinib. Gene expression was normalized to *Hprt1*, and the level was arbitrarily set to 1 in untreated osteoclasts. (**F**) Osteoclasts were grown on dentine discs and bone resorption was analyzed by toluidine-blue staining and image analysis. Data are normalized to the level of untreated osteoclasts. (**G** and **H**) Osteoclasts were differentiated in the presence of EGF. At day 7, (G) TRAP activity was measured by an enzymatic reaction and (H) the number of osteoclasts per well was counted. (**I**) Osteoclasts were pretreated with either erlotinib (5 μM) or PD153035 (5 μM) and stimulated with EGF (50 ng/ml) for 5 min and Western blots were performed. (**J**) Monocytes were treated with serum-free differentiation media containing M-CSF and RANKL for 45 min (45 m) or 6 h (6 h). *Fos* expression was determined by quantitative PCR. (B–D and G–J) Data represent one experiment of at least three independent experiments. (E and F) Data represent one experiment of at least two independent experiments. (A and B) Scale bars, 150 μm. Error bars indicate ± SEM. For all experiments: $*p < 0.05$, $**p < 0.01$, $***p < 0.001$. OC, Osteoclast.

Downloaded from www.jimmunol.org on April 4, 2012

for these experiments because suboptimal osteoclast formation was required to discriminate the effects of EGF. EGF significantly increased the cells' TRAP activity and the number of osteoclasts formed, suggesting that it promotes osteoclastogenesis. Moreover, concurrent treatment with erlotinib blocked the increase in TRAP activity and formation of osteoclasts induced by EGF, and partially blocked the TRAP activity induced by RANKL alone (Fig. 5G, 5H).

EGF induced the phosphorylation of EGFR, Akt, and Erk1/2 in osteoclasts, and this was reduced by treatment with erlotinib and PD153035 (Fig. 5I), suggesting that erlotinib suppresses osteoclastogenesis by inhibiting EGFR-induced gene expression. FOS is a member of the AP-1 family of transcription factors and is required for osteoclast formation (37). RANKL activates *c-Fos* transcription (37), possibly by transactivating EGFR (38). Moreover, EGFR signaling independently upregulates *c-Fos* expression in HeLa cells (39). We therefore tested the effect of erlotinib on monocytes incubated with differentiation media containing M-CSF and RANKL. We found that the osteoclast differentiation media caused a strong upregulation of *Fos* mRNA expression at 6 h, and that this was reduced by erlotinib (Fig. 5J). Given that FOS is necessary for osteoclast development (37), inhibiting FOS may be one way in which erlotinib reduces osteoclastogenesis.

Discussion

In this study, we show that EGF levels are abnormally high in the serum of RA patients, and that EGFR is both highly expressed and activated in synovial tissue from RA patients and from mice with autoimmune arthritis. Moreover, we find that the EGFR inhibitor erlotinib attenuates autoimmune arthritis in mice, reducing synovitis, pannus formation, and cartilage and bone erosion in their synovial joints. Erlotinib-induced attenuation of autoimmune arthritis was associated with a reduction in number of osteoclasts and blood vessels formed in the mouse paws, and erlotinib directly inhibited the formation of osteoclasts and the proliferation of endothelial cells in vitro, as did a distinct EGFR inhibitor. Erlotinib also inhibited the proliferation and cytokine production of synovial fibroblasts in vitro, an effect that may explain its ability to reduce pannus formation and synovitis in vivo.

Previous findings are conflicting as to which EGFR ligand is upregulated in RA. Studies of bone marrow-derived mononuclear cells and synovial fluid have implicated EGF, TGF-α, and amphiregulin in RA (9, 12, 40, 41). However, we find that only levels of EGF and betacellulin, and not TGF-α, HB-EGF, or amphiregulin, are higher in serum from RA patients than in serum from healthy individuals. This suggests that the exact EGF ligand involved in RA may differ between serum and synovial fluid, or may depend on RA subtype, disease duration, or the treatment regimen. Although we focused on EGF in this study, it will be interesting to further define the activity of betacellulin in RA. Betacellulin is known to promote angiogenesis, indicating that it may promote the growth of the synovium (42).

Previous studies found that EGFR is expressed on RA fibroblast cell lines and on the vascular endothelial cells and subsynovial fibroblasts of certain RA patients (9, 10). In this study, we show that EGFR is not only expressed but also activated in RA and CIA synovium. Furthermore, we confirm that EGFR is expressed and can be transactivated by EGF in cultured synovial fibroblasts.

Our finding that erlotinib, an EGFR inhibitor that is Food and Drug Administration approved for the treatment of cancer, attenuated CIA complements a recent report indicating that soluble herstatin, which inhibits the dimerization of ErbB receptors, attenuates CIA (6). Taken together, these findings suggest that inhibition of EGFR, and possibly ErbB2 (which is a frequent binding partner of EGFR), may provide benefit in RA.

Amphiregulin has been shown to increase the proliferation of RA synovial fibroblasts and to increase their expression of VEGF, IL-8, GM-CSF, and IL-6 (9, 40). EGF on its own was found to have little effect on synovial fibroblasts, but to synergize with TNF and IL-1β to increase mRNA expression of MMPs and proinflammatory molecules (19). We find that EGF alone can in fact induce the proliferation of synovial fibroblasts in a dose-dependent manner, an effect that could promote the growth of the pannus in RA. Moreover, we demonstrate that EGF alone can induce the production of IL-8, VEGF, MMP-3, and MCP-1 protein by RA synovial fibroblasts, and that concurrent EGFR inhibition with erlotinib or PD153035 reduces the production of these factors. Thus, erlotinib may indirectly have widespread effects on RA through its actions on RA synovial fibroblasts. These include decreasing IL-8– and MCP-1–induced neutrophil and monocyte migration into the joint space (23, 24), decreasing angiogenesis driven by VEGF (22), and reducing cartilage destruction promoted by MMP-3 (25).

RA synovium contains significantly greater numbers of blood vessels than does osteoarthritis synovium (26). In this study, we demonstrate that erlotinib reduces the number of blood vessels in CIA and that this may occur through both direct and indirect mechanisms. Erlotinib may directly reduce angiogenesis by impeding endothelial cell proliferation and COX-2 expression, and indirectly reduce angiogenesis by decreasing VEGF production by RA synovial fibroblasts.

RA and CIA are characterized by the progressive destruction of bone and cartilage in the synovial joints, a process mediated by osteoclasts (34, 35). Osteoclast development is driven by excessive production of RANKL and TNF in the RA synovium, which interact with their receptors on monocytes and macrophages driving osteoclast formation through the expression of transcription factors, such as FOS of the AP-1 complex and NFATc1 (4). EGF and EGFR may also promote bone destruction in RA, as bone formation is abnormal in EGFR-deficient mice, suggesting that EGFR is important for osteoclast formation (43). The EGFR inhibitors AG1478 and PD153035 have been shown to reduce osteoclast formation (38, 43); in this study, we show that EGFR inhibition with erlotinib also reduces osteoclast formation. EGFR inhibition reduced the number of osteoclasts formed, as well as their size, osteoclast-specific gene expression, and bone resorption capacity. Moreover, we demonstrate that EGF increases the TRAP enzymatic activity and number of osteoclasts formed during low-RANKL conditions. This indicates that EGF, similar to TNF, promotes osteoclast activity in RA and CIA. Erlotinib reduced the osteoclast activity induced by EGF as well as that induced in the absence of added EGF. Furthermore, we demonstrate that erlotinib acts on osteoclasts by reducing EGF-induced phosphorylation of EGFR, Erk, and Akt, as well as RANKL-induced FOS expression. EGF may therefore supplement the transactivation of EGFR by RANKL and thereby promote osteoclast formation. This is important because it indicates that EGFR, in addition to RANK, might be a beneficial target to reduce bone loss in RA.

Taken together, our findings suggest that targeting EGFR has potential as a novel therapeutic strategy for RA. Rational targeting of EGFR inhibitors to specific phases of RA, limiting the duration of dosing, and combining EGFR inhibitors with other disease-modifying agents may be important in maximizing the benefit of EGFR inhibitors in RA. Patients with early, active RA may benefit most from EGFR inhibitor therapy. Patients with undifferentiated arthritis who go on to develop RA exhibit a distinct and transient increase in EGF expression in synovial fluid (44). This

Downloaded from www.jimmunol.org on April 4, 2012

suggests that early in the course of arthritis there may be a window of opportunity where EGFR inhibition could be beneficial in those patients with significantly heightened EGF levels. EGF levels may also correlate with disease activity and severity. EGF levels in synovial fluid correlated with C-reactive protein and IgM levels in RA patients (12). High pretreatment levels of EGF and MCP-1 distinguished patients who responded to etanercept therapy (45). Thus, as disease progresses, EGFR inhibition may continue to be of benefit to RA patients with more destructive disease courses.

EGFR inhibitors such as erlotinib are known to cause adverse side effects, for example, rash and diarrhea (13), which make them less amenable to treating chronic, nonterminal diseases such as RA. However, several treatment strategies may increase the tolerability and efficacy of EGFR inhibitor therapy. First, pulsed, rather than chronic, therapy may suffice during early disease or during a disease flare when EGF levels appear to peak. Second, patients with high levels of EGFR ligands in their serum may be specifically targeted for EGFR inhibitor therapy. Third, next-generation EGFR inhibitors being developed for the treatment of cancer may have a better therapeutic index. These include agents that bind EGFR irreversibly, target multiple ErbB family members, and inhibit additional kinases receptors such as those for VEGF and fibroblast growth factor, which are known to drive disease (46).

In conclusion, we show that EGFR inhibition using erlotinib reduces the severity of autoimmune arthritis in mice. The mechanism of action appears to be through inhibition of synovial fibroblast, endothelial cell, and osteoclast inflammatory and degradative responses. Our findings demonstrate the importance of EGFR in the pathogenesis of autoimmune arthritis, and they provide evidence that EGFR, a molecule long targeted in cancer, should be considered a new molecular target in RA.

Acknowledgments

We thank members of the Robinson laboratory for many rewarding discussions. Lauren Lahey, Orr Sharpe, and Yann Chong Tan particularly aided in figure development, Western blots, and PCR troubleshooting, respectively. Eun-Ju Chang and Qian Wang provided valuable insight on osteoclast development and analysis, and the Butcher Laboratory members generously supplied endothelial cell resources and knowledge.

Disclosures

The authors have no financial conflicts of interest.

References

1. Cope, A. P. 2008. T cells in rheumatoid arthritis. *Arthritis Res. Ther.* 10(Suppl. 1): S1.
2. Scott, D. L., F. Wolfe, and T. W. Huizinga. 2010. Rheumatoid arthritis. *Lancet* 376: 1094–1108.
3. Firestein, G. S. 1999. Starving the synovium: angiogenesis and inflammation in rheumatoid arthritis. *J. Clin. Invest.* 103: 3–4.
4. Schett, G. 2007. Cells of the synovium in rheumatoid arthritis: osteoclasts. *Arthritis Res. Ther.* 9: 203.
5. Sullivan, T., C. G. Benjamin, P. W. Kempf, and J. F. Deeken. 2010. Cetuximab in the treatment of rheumatoid arthritis. *J. Clin. Rheumatol.* 16: 32–33.
6. Sumariwalla, P. F., P. Jin, J. Zhang, I. Ni, D. Crawford, H. M. Shepard, E. M. Paleolog, and M. Feldmann. 2008. Antagonism of the human epidermal growth factor receptor family controls disease severity in murine collagen-induced arthritis. *Arthritis Rheum.* 58: 3071–3080.
7. Gompels, L. L., N. M. Malik, L. Madden, P. Jin, M. Feldmann, H. M. Shepard, and E. M. Paleolog. 2011. Human epidermal growth factor receptor bispecific ligand trap RB200: abrogation of collagen-induced arthritis in combination with tumour necrosis factor blockade. *Arthritis Res. Ther.* 13: R161.
8. Herbst, R. S. 2004. Review of epidermal growth factor receptor biology. *Int. J. Radiat. Oncol. Biol. Phys.* 59(2, Suppl)21–26.
9. Yamane, S., S. Ishida, Y. Hanamoto, K. Kumagai, R. Masuda, K. Tanaka, N. Shiobara, N. Yamane, T. Mori, T. Juji, et al. 2008. Proinflammatory role of amphiregulin, an epidermal growth factor family member whose expression is augmented in rheumatoid arthritis patients. *J. Inflamm. (Lond.)* 5: 5.
10. Young, C. L., T. C. Adamson, III, J. H. Vaughan, and R. I. Fox. 1984. Immunohistologic characterization of synovial membrane lymphocytes in rheumatoid arthritis. *Arthritis Rheum.* 27: 32–39.
11. Farahat, M. N., G. Yanni, R. Poston, and G. S. Panayi. 1993. Cytokine expression in synovial membranes of patients with rheumatoid arthritis and osteoarthritis. *Ann. Rheum. Dis.* 52: 870–875.
12. Kusada, J., T. Otsuka, N. Matsui, T. Hirano, K. Asai, and T. Kato. 1993. Immuno-reactive human epidermal growth factor (h-EGF) in rheumatoid synovial fluids. *Nippon Seikeigeka Gakkai Zasshi* 67: 859–865.
13. Lu, J. F., S. M. Eppler, J. Wolf, M. Hamilton, A. Rakhit, R. Bruno, and B. L. Lum. 2006. Clinical pharmacokinetics of erlotinib in patients with solid tumors and exposure-safety relationship in patients with non-small cell lung cancer. *Clin. Pharmacol. Ther.* 80: 136–145.
14. Paniagua, R. T., O. Sharpe, P. P. Ho, S. M. Chan, A. Chang, J. P. Higgins, B. H. Tomooka, F. M. Thomas, J. J. Song, S. B. Goodman, et al. 2006. Selective tyrosine kinase inhibition by imatinib mesylate for the treatment of autoimmune arthritis. *J. Clin. Invest.* 116: 2633–2642.
15. Higgins, B., K. Kolinsky, M. Smith, G. Beck, M. Rashed, V. Adames, M. Linn, E. Wheeldon, L. Gand, H. Birnboeck, and G. Hoffmann. 2004. Antitumor activity of erlotinib (OSI-774, Tarceva) alone or in combination in human non-small cell lung cancer tumor xenograft models. *Anticancer Drugs* 15: 503–512.
16. Hidalgo, M., and D. Bloedow. 2003. Pharmacokinetics and pharmacodynamics: maximizing the clinical potential of Erlotinib (Tarceva). *Semin. Oncol.* 30(3, Suppl. 7)25–33.
17. Abeles, A. M., and M. H. Pillinger. 2006. The role of the synovial fibroblast in rheumatoid arthritis: cartilage destruction and the regulation of matrix metalloproteinases. *Bull. NYU Hosp. Jt. Dis.* 64: 20–24.
18. Goddard, D. H., S. L. Grossman, and M. E. Moore. 1990. Autocrine regulation of rheumatoid arthritis synovial cell growth in vitro. *Cytokine* 2: 149–155.
19. Huber, L. C., P. Künzler, S. H. Boyce, B. A. Michel, R. E. Gay, B. S. Ink, and S. Gay. 2008. Effects of a novel tyrosine kinase inhibitor in rheumatoid arthritis synovial fibroblasts. *Ann. Rheum. Dis.* 67: 389–394.
20. Taylor, D. J., M. Feldmann, J. M. Evanson, and D. E. Woolley. 1989. Comparative and combined effects of transforming growth factors α and α, interleukin-1 and interferon-gamma on rheumatoid synovial cell proliferation, glycolysis and prostaglandin E production. *Rheumatol. Int.* 9: 65–70.
21. Nah, S. S., H. J. Won, E. Ha, I. Kang, H. Y. Cho, S. J. Hur, S. H. Lee, and H. H. Baik. 2010. Epidermal growth factor increases prostaglandin E_2 production via ERK1/2 MAPK and NF-κB pathway in fibroblast like synoviocytes from patients with rheumatoid arthritis. *Rheumatol. Int.* 30: 443–449.
22. Maruotti, N., F. P. Cantatore, E. Crivellato, A. Vacca, and D. Ribatti. 2006. Angiogenesis in rheumatoid arthritis. *Histol. Histopathol.* 21: 557–566.
23. Endo, H., T. Akahoshi, K. Takagishi, S. Kashiwazaki, and K. Matsushima. 1991. Elevation of interleukin-8 (IL-8) levels in joint fluids of patients with rheumatoid arthritis and the induction by IL-8 of leukocyte infiltration and synovitis in rabbit joints. *Lymphokine Cytokine Res.* 10: 245–252.
24. Ogata, H., M. Takeya, T. Yoshimura, K. Takagi, and K. Takahashi. 1997. The role of monocyte chemoattractant protein-1 (MCP-1) in the pathogenesis of collagen-induced arthritis in rats. *J. Pathol.* 182: 106–114.
25. Ainola, M. M., J. A. Mandelin, M. P. Liljeström, T. F. Li, M. V. Hukkanen, and Y. T. Konttinen. 2005. Pannus invasion and cartilage degradation in rheumatoid arthritis: involvement of MMP-3 and interleukin-1β. *Clin. Exp. Rheumatol.* 23: 644–650.
26. FitzGerald, O., M. Soden, G. Yanni, R. Robinson, and B. Bresnihan. 1991. Morphometric analysis of blood vessels in synovial membranes obtained from clinically affected and unaffected knee joints of patients with rheumatoid arthritis. *Ann. Rheum. Dis.* 50: 792–796.
27. Wu, L. W., L. D. Mayo, J. D. Dunbar, K. M. Kessler, M. R. Baerwald, E. A. Jaffe, D. Wang, R. S. Warren, and D. B. Donner. 2000. Utilization of distinct signaling pathways by receptors for vascular endothelial cell growth factor and other mitogens in the induction of endothelial cell proliferation. *J. Biol. Chem.* 275: 5096–5103.
28. Mehta, V. B., and G. E. Besner. 2007. HB-EGF promotes angiogenesis in endothelial cells via PI3-kinase and MAPK signaling pathways. *Growth Factors* 25: 253–263.
29. Mehta, V. B., Y. Zhou, A. Radulescu, and G. E. Besner. 2008. HB-EGF stimulates eNOS expression and nitric oxide production and promotes eNOS dependent angiogenesis. *Growth Factors* 26: 301–315.
30. Semino, C. E., R. D. Kamm, and D. A. Lauffenburger. 2006. Autocrine EGF receptor activation mediates endothelial cell migration and vascular morphogenesis induced by VEGF under interstitial flow. *Exp. Cell Res.* 312: 289–298.
31. Baraf, H. S. 2007. Efficacy of the newest COX-2 selective inhibitors in rheumatic disease. *Curr. Pharm. Des.* 13: 2228–2236.
32. Siegle, I., T. Klein, J. T. Backman, J. G. Saal, R. M. Nüsing, and P. Fritz. 1998. Expression of cyclooxygenase 1 and cyclooxygenase 2 in human synovial tissue: differential elevation of cyclooxygenase 2 in inflammatory joint diseases. *Arthritis Rheum.* 41: 122–129.
33. Woods, J. M., A. Mogollon, M. A. Amin, R. J. Martinez, and A. E. Koch. 2003. The role of COX-2 in angiogenesis and rheumatoid arthritis. *Exp. Mol. Pathol.* 74: 282–290.
34. Choi, Y., J. R. Arron, and M. J. Townsend. 2009. Promising bone-related therapeutic targets for rheumatoid arthritis. *Nat Rev Rheumatol* 5: 543–548.
35. Choi, S., Y. A. Lee, S. J. Hong, G. J. Lee, S. W. Kang, J. H. Park, and H. K. Park. 2011. Evaluation of inflammatory change and bone erosion using a murine type II collagen-induced arthritis model. *Rheumatol. Int.* 31: 595–603.
36. Rho, J., C. R. Altmann, N. D. Socci, L. Merkov, N. Kim, H. So, O. Lee, M. Takami, A. H. Brivanlou, and Y. Choi. 2002. Gene expression profiling of

Downloaded from www.jimmunol.org on April 4, 2012

osteoclast differentiation by combined suppression subtractive hybridization (SSH) and cDNA microarray analysis. *DNA Cell Biol.* 21: 541–549.
37. Boyce, B. F., T. Yamashita, Z. Yao, Q. Zhang, F. Li, and L. Xing. 2005. Roles for NF-κB and c-Fos in osteoclasts. *J. Bone Miner. Metab.* 23(Suppl.): 11–15.
38. Yi, T., H. L. Lee, J. H. Cha, S. I. Ko, H. J. Kim, H. I. Shin, K. M. Woo, H. M. Ryoo, G. S. Kim, and J. H. Baek. 2008. Epidermal growth factor receptor regulates osteoclast differentiation and survival through cross-talking with RANK signaling. *J. Cell. Physiol.* 217: 409–422.
39. Leaman, D. W., S. Pisharody, T. W. Flickinger, M. A. Commane, J. Schlessinger, I. M. Kerr, D. E. Levy, and G. R. Stark. 1996. Roles of JAKs in activation of STATs and stimulation of c-fos gene expression by epidermal growth factor. *Mol. Cell. Biol.* 16: 369–375.
40. Nakamura, N., Y. Shimaoka, T. Tougan, H. Onda, D. Okuzaki, H. Zhao, A. Fujimori, N. Yabuta, I. Nagamori, A. Tanigawa, et al. 2006. Isolation and expression profiling of genes upregulated in bone marrow-derived mononuclear cells of rheumatoid arthritis patients. *DNA Res.* 13: 169–183.
41. Hallbeck, A. L., T. M. Walz, K. Briheim, and A. Wasteson. 2005. TGF-α and ErbB2 production in synovial joint tissue: increased expression in arthritic joints. *Scand. J. Rheumatol.* 34: 204–211.
42. Kim, H. S., H. S. Shin, H. J. Kwak, C. H. Cho, C. O. Lee, and G. Y. Koh. 2003. Betacellulin induces angiogenesis through activation of mitogen-activated protein kinase and phosphatidylinositol 3′-kinase in endothelial cell. *FASEB J.* 17: 318–320.
43. Wang, K., H. Yamamoto, J. R. Chin, Z. Werb, and T. H. Vu. 2004. Epidermal growth factor receptor-deficient mice have delayed primary endochondral ossification because of defective osteoclast recruitment. *J. Biol. Chem.* 279: 53848–53856.
44. Raza, K., F. Falciani, S. J. Curnow, E. J. Ross, C. Y. Lee, A. N. Akbar, J. M. Lord, C. Gordon, C. D. Buckley, and M. Salmon. 2005. Early rheumatoid arthritis is characterized by a distinct and transient synovial fluid cytokine profile of T cell and stromal cell origin. *Arthritis Res. Ther.* 7: R784–R795.
45. Fabre, S., A. M. Dupuy, N. Dossat, C. Guisset, J. D. Cohen, J. P. Cristol, J. P. Daures, and C. Jorgensen. 2008. Protein biochip array technology for cytokine profiling predicts etanercept responsiveness in rheumatoid arthritis. *Clin. Exp. Immunol.* 153: 188–195.
46. Gazdar, A. F. 2010. Epidermal growth factor receptor inhibition in lung cancer: the evolving role of individualized therapy. *Cancer Metastasis Rev.* 29: 37–48.

Downloaded from www.jimmunol.org on April 4, 2012